

Superconductivity induced by aging and annealing in $K_{1-\delta}Cr_3As_3H_x$

Jin-Jin Xiang,^{1,*} Ya-Long Yu,^{1,*} Si-Qi Wu,¹ Bai-Zhuo Li,¹ Ye-Ting Shao,¹ Zhang-Tu Tang,²
Jin-Ke Bao,³ and Guang-Han Cao^{1,4,5,†}

¹Department of Physics and Zhejiang Province Key Laboratory of Quantum Technology and Devices,
Zhejiang University, Hangzhou 310027, China

²College of Physics and Electronic Information Engineering, Zhejiang Normal University, Jinhua 321004, China

³Materials Science Division, Argonne National Laboratory, Argonne, Illinois 60439, USA

⁴State Key Laboratory of Silicon Materials, Zhejiang University, Hangzhou 310027, China

⁵Collaborative Innovation Centre of Advanced Microstructures, Nanjing University, Nanjing 210093, China



(Received 13 August 2019; published 12 November 2019)

There has been a puzzling discrepancy on the physical property of quasi-one-dimensional Cr-based compound KCr_3As_3 . While the polycrystalline KCr_3As_3 was originally reported to be nonsuperconducting with a spin-glass ground state, the single-crystalline KCr_3As_3 was later found to exhibit superconductivity at ~ 5 K. Here we demonstrate that both the polycrystals and single crystals can be made either nonsuperconducting or superconducting. The pristine samples show a spin-glass behavior only, and superconductivity below 5 K is actually induced by the post-aging and/or post-annealing. The result can be understood in terms of hydrogen intercalation into the one-dimensional Cr_3As_3 tubes, which was discovered very recently by K. M. Taddei *et al.* (arXiv:1905.03360). In addition, significant K deficiency and microscopic inhomogeneity have been revealed, suggesting a phase separation scenario with columnar superconductivity in $K_{1-\delta}Cr_3As_3H_x$. The possible processes of the hydrogen intercalation are given.

DOI: [10.1103/PhysRevMaterials.3.114802](https://doi.org/10.1103/PhysRevMaterials.3.114802)

I. INTRODUCTION

The quasi-one-dimensional chromium-based arsenide $K_2Cr_3As_3$ [1] has attracted considerable research interest in recent years primarily because of the possible spin-triplet unconventional superconductivity [2–8]. The crystal structure of $K_2Cr_3As_3$ is characterized by the linear chain, $[(Cr_3As_3)^{2-}]_{\infty}$, a double-walled subnanotube [see Fig. 1(a)]. Replacement of the counterion K^+ with Rb^+ [9], Cs^+ [10], or Na^+ [11] brings about superconductivity as well. The superconducting transition temperatures (T_c 's) of $A_2Cr_3As_3$ ($A = Na, K, Rb,$ and Cs) are 8.6, 6.1, 4.8, and 2.2 K, respectively.

There exist the cousin compounds, 133-type ACr_3As_3 ($A = K, Rb,$ and Cs), which were obtained by removing half of the A^+ ions from the 233-type $A_2Cr_3As_3$ through an ethanol bath at room temperature [12,13]. The soft-chemical reaction is topotactic, keeping the $(Cr_3As_3)_{\infty}$ chains intact [Figs. 1(b)–1(d)]. The resultant 133-type polycrystalline samples were first reported to be nonsuperconductive with a spin-glass ground state [12–14]. Two years later, however, Ren and co-workers [15] reported superconductivity at ~ 5 K in the post-treated KCr_3As_3 single crystals. Then, superconductivity at 7.3 K was observed in $RbCr_3As_3$ single crystals by the same group [16]. The latter result basically excludes the possibility that superconductivity could be from the trace remaining $Rb_2Cr_3As_3$ in the sample, since the T_c of bulk $Rb_2Cr_3As_3$ is

only 4.8 K [9]. Nevertheless, no superconductivity has so far been reported for the third 133-type member, $CsCr_3As_3$.

The conflicting result between the polycrystals and single crystals of ACr_3As_3 is very puzzling. Ren and co-workers [15] explained the absence of superconductivity in polycrystals as a result of disorder and poor crystallinity. In polycrystals, however, the microscopic disorder and crystallinity of the crystallites is generally similar to that of the corresponding single crystals, provided their synthetic conditions are similar. As an example, the T_c value is almost the same for the polycrystals and the single crystals of $K_2Cr_3As_3$ [1]. Additionally, the KCr_3As_3 crystal shows similarly high upper critical fields [15] which suggest short superconducting coherence lengths (a few nanometers [17]) that are much smaller than the crystallite size in the polycrystals. Therefore, superconductivity should have also been observed in the KCr_3As_3 polycrystals. To clarify the discrepancy, we reinvestigated the 133-type system by finely controlling the post-treatments. We found that the pristine KCr_3As_3 crystals were actually not superconducting. Superconductivity emerges either with aging in ethanol or by post-annealing at a mildly elevated temperature. The case for the polycrystals is basically similar, but annealing turns out to be much more effective (than aging) for inducing superconductivity.

It was not easy to understand the aging and annealing effects, but very recently, with neutron diffractions, Taddei *et al.* [18] revealed that hydrogen was incorporated into the KCr_3As_3 lattice, which had been missed in the previous studies [12,15]. The neutron-diffraction result indicates that hydrogen atoms partially occupy the $2b$ (0,0,0) site which is located at the center of the Cr_6 octahedra [Figs. 1(b),

*These authors contributed equally to this work.

†ghcao@zju.edu.cn

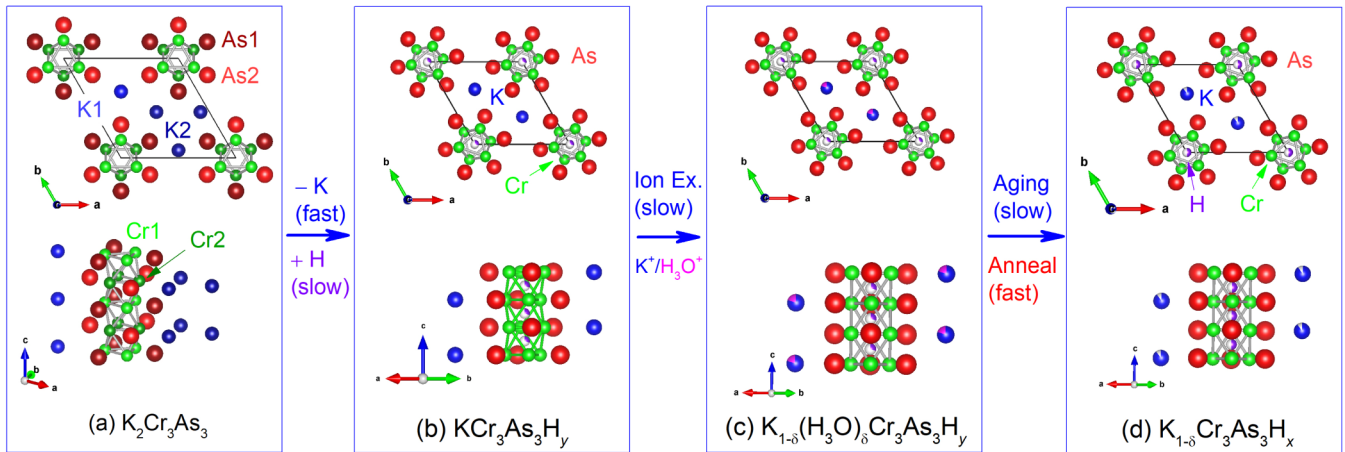


FIG. 1. Schematic representation of phase conversions from $\text{K}_2\text{Cr}_3\text{As}_3$ (a) to the 133-type variants that take the form of (b), (c), or (d). Panel (b) represents the pristine compound, $\text{KCr}_3\text{As}_3\text{H}_y$, in which a small amount of hydrogen is present at the $2b$ site (0,0,0) within the Cr_3 tubes [18]. Panel (c) depicts an intermediate product as a result of ion exchange between K^+ and H_3O^+ . Panel (d) describes the superconductive object with more hydrogen incorporated after aging and/or annealing.

1(c), and 1(d)]. The H occupancy is 0.35 for the as-prepared 133-type polycrystalline powders which show a spin-glass behavior with a trace superconducting signature. With the post-ethanol-thermal treatment, the H occupancy increases to 0.65–0.71, and superconductivity at around 4.5 K emerges with $\sim 80\%$ full diamagnetism in the zero-field-cooling (ZFC) mode. It was then concluded that the difference between the as-prepared and the post-treated samples was not a change in crystallinity but in the H intercalation, which may dope extra electrons for inducing superconductivity [18,19].

Nevertheless, how hydrogen enters the lattice remains illusive. It was tentatively proposed that the remaining ethanol molecules substitute onto the K site or intercalate into the lattice, and the post-treatment forces more H into the material [18]. This mechanism seems to be questionable. First, the incorporation of $\text{C}_2\text{H}_5\text{OH}$ would expand the lattice remarkably, which is not the case. Second, from the chemistry point of view, it is very unlikely for KCr_3As_3 to react with $\text{C}_2\text{H}_5\text{OH}$, forming $\text{KH}_x\text{Cr}_3\text{As}_3$ (which means that ethanol can hydrogenate KCr_3As_3). In this paper we report the details of the aging and annealing effects which can be basically understood in terms of H intercalation. A plausible mechanism of the H intercalation is proposed, with which the different aging behaviors between the polycrystals and the single crystals can be explained.

II. EXPERIMENTAL METHODS

The preparations of the pristine 133-type polycrystalline and single-crystalline samples were similar to those of the previous reports [12,15], but the post-treatments were modified and strictly controlled. In the previous preparations, the aging and/or annealing processes had actually been involved already [12,15,18]. Here the experiments were specially designed to highlight the post-treatment effect, and to distinguish the aging effect from the post-annealing one as well. First, $\text{K}_2\text{Cr}_3\text{As}_3$ polycrystals and crystals were synthesized, according to the procedures reported previously [1].

Second, pristine 133-type samples were obtained by soaking the $\text{K}_2\text{Cr}_3\text{As}_3$ polycrystalline pellets or single crystals (about $0.1 \times 0.1 \times 3 \text{ mm}^3$ in size) in ethanol (AR, 99%) at room temperature till no hydrogen gas escaped from the liquid. The reaction takes only 1–2 hours (2–12 hours, depending on the sample's size) for the single crystals (polycrystals), which was supported by the time dependence of the volume of H_2 gas released (see Fig. S1 in the Supplemental Material (SM) [20]). Third, the pristine samples were aged in ethanol at room temperature with durations from 1 day up to 1 year. Finally, the pristine samples and the aged samples were annealed at 80–100 °C in vacuum for 5–12 hours. We found that the pristine and short-time-aged polycrystalline sample (dried by evacuation) heats up by itself when exposed in air. Also, when it was soaked in water, hydrogen gas bubbles escaped again, and the 133-type phase remained afterward. These observations help to understand the H-intercalation process, which will be discussed later on. By contrast, the final superconductive samples are basically air stable over several weeks.

Powder x-ray diffraction (XRD) experiments were performed at room temperature on a PANalytical x-ray diffractometer (Empyrean model) with a $\text{CuK}\alpha_1$ monochromator. The lattice parameters were calculated with least-squares fitting using about 15 reflections, and calibration with a Si internal standard was employed. The energy-dispersive x-ray spectra (EDXS) were collected on an Octane Plus Detector (AMETEX EDAX) equipped in a field-emitting scanning electron microscope (SEM; Hitachi S-4800). With the EDXS, the atomic percentages of K, Cr, and As were obtained using the K lines by the eZAF Smart Quant analysis. The dc magnetic susceptibility was measured on a Quantum Design magnetic property measurement system (MPMS3). Both the ZFC and field-cooling (FC) protocols were employed. For the rodlike single crystals, the applied field was along the rod direction, and for the bar-shaped polycrystals, the external field was also along the bar direction, such that the demagnetization effect was insignificant.

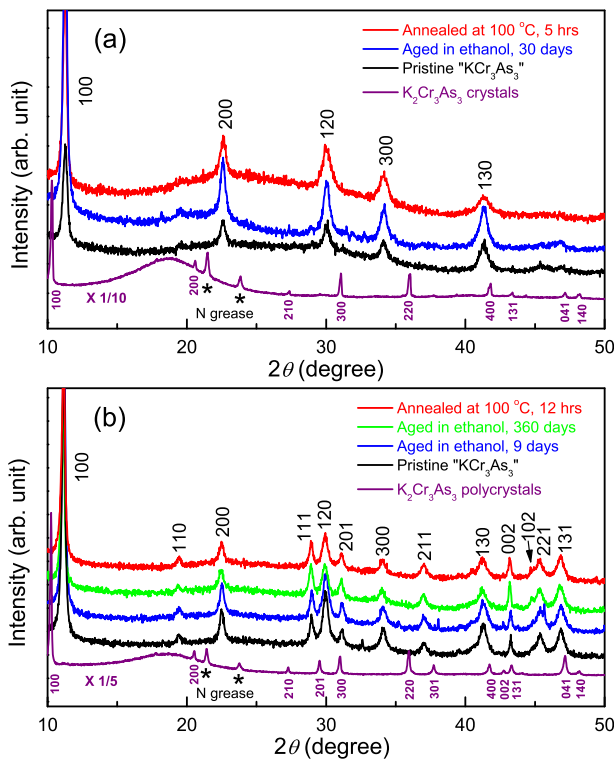


FIG. 2. Powder x-ray diffraction patterns for the pristine and the post-treated KCr_3As_3 single-crystalline (a) and polycrystalline (b) samples. The XRD data of $\text{K}_2\text{Cr}_3\text{As}_3$ crystals and polycrystals (protected with coating N grease) are presented for comparison.

III. EXPERIMENTAL RESULTS

A. XRD and EDXS results

First of all, the pristine and the post-treated samples were characterized by the experiments of XRD, SEM, and EDXS. Figure 2 shows powder XRD patterns of the 233-type $\text{K}_2\text{Cr}_3\text{As}_3$ as well as the 133-type KCr_3As_3 samples. After $\text{K}_2\text{Cr}_3\text{As}_3$ was soaked in ethanol for 1 hour (12 hours) for the crystals (polycrystals), $\text{K}_2\text{Cr}_3\text{As}_3$ changed completely into KCr_3As_3 , the latter of which is called *pristine* 133-type material (hereafter “133” is termed the KCr_3As_3 variants with the similar lattice constants). Note that for the single-crystalline samples (being ground slightly before loading onto the sample holder), only $(hk0)$ reflections show up, because the rodlike crystallites mostly lie flat on the sample holder. The above result, together with the measurement of hydrogen-gas volume (Fig. S1 in the SM [20]), indicates that the K-deintercalation reaction from “233” to “133” is actually much faster than expected (in previous literature [12,15,18], as a comparison, the K-deintercalation process took 5–7 days).

With the post-aging or post-annealing, the XRD patterns hardly change at first sight. All the diffractions can be well indexed with the unit cell of KCr_3As_3 ($a \approx 9.09 \text{ \AA}$ and $c \approx 4.18 \text{ \AA}$) [12], verifying that the 133-type phase remains. The post-treatment subtly changes the lattice parameters, which will be discussed in the following section.

Important to note is that the diffraction peaks for the 133-type crystals and polycrystals are unusually broad. Similar results were reported previously [12,15,18]. The full width at

half maximum (FWHM) of the (300) reflection of the pristine 133 crystals, for example, is as large as 0.43° , in comparison with the normal FWHM of 0.14° for the (300) reflection of the 233-type $\text{K}_2\text{Cr}_3\text{As}_3$ crystals. The FWHM value tends to increase with aging and/or annealing. The case is similar for the 133-type polycrystals, yet the (002) peak is exclusively narrower [Fig. 2(b)]. The diffraction-peak broadening is generally attributed to the effects of strain, crystallinity, and crystalline size [18]. We previously considered the anisotropic crystallite-size effect for understanding the diffraction broadening for most reflections other than $(00l)$ [12]. However, the SEM images (see the insets of Fig. S2 in the SM [20]) show that the wirelike crystallites of the polycrystals are 1–2 μm thick and the thickness of the rodlike crystals is mostly larger than 10 μm , both of which do not account for the large peak broadening. The SEM images also indicate that the crystallites are basically not bent, which means insignificant anisotropic microscopic strain. Then, the $(hk0)$ broadening should mostly come from the poor crystallinity (mainly within ab planes) that is possibly associated with the compositional inhomogeneity at a micrometer scale. Note that the crystallinity, if evaluated with the FWHM values, becomes even poorer after aging or annealing.

We carefully examined the chemical composition of the 133-series samples by the EDXS measurement. First of all, the chemical composition of the surface of the pristine crystals is close to the stoichiometry of KCr_3As_3 (see Fig. S2(a) in the SM [20]). However, the K content of the crushed crystals varies from 0.98 to 1.14, indicating compositional inhomogeneity at least on a micrometer scale. Second, after the pristine crystals are aged in an ethanol bath for 30 days, the K content clearly decreases Fig. S2(b). Also, the K content is more inhomogeneous, ranging from 0.72 to 0.95. Finally, the annealed samples also show spatial inhomogeneity in K content. Almost stoichiometric composition was measured on some spots (see Table S1 in the SM [20] for the details). The compositional inhomogeneity in K content suggests the existence of phase separation, which leads to the XRD peak broadening above.

Similar changes in K content were observed for the 133-type polycrystalline samples. The pristine polycrystals show almost stoichiometric composition of KCr_3As_3 , consistent with our earlier report [12]. After the ethanol bath for 7–30 days, the K content decreases to 0.7–0.9. Again, the K content was found to be inhomogeneous: different areas/spots in the identical sample show different K content (Fig. S2(d) in the SM [20]). Table I briefly summarizes the chemical compositions of the pristine and post-treated 133-type samples (the detailed EDXS results are presented in Tables S1 and S2 of the SM [20]). As can be seen, both the Cr content and the As content converge to the stoichiometry. However, the K content appears to be scattered for all the samples. On average, the K content is around 1.0 for the pristine samples but for the aged and annealed samples, the K content is substantially reduced to about 0.8.

We tried to detect the possible K vacancies using the Rietveld analyses on the XRD data of the pristine, aged, and annealed samples. The Rietveld refinements showed that in all the cases, the K content is very close to 1.0, independent of the post-treatments. This result is consistent with those

TABLE I. Statistics on the chemical compositions of the pristine and post-treated samples of KCr_3As_3 obtained from the EDXS measurements. The Cr content is set to be 3.00, according to the expected chemical formula. The aged samples refer to the pristine ones that remained in ethanol bath at room temperature for 1–4 weeks. The annealed samples are the aged ones that were annealed at 80–100 °C for 5–12 hours. The numbers in parentheses denote the measurement uncertainty. Note that the As content has $\sim 10\%$ positive deviation due to the instrumental systematic error [12].

Samples/Elements	K	Cr	As
Pristine crystals	0.98–1.14(6)	3.00	3.0–3.3(2)
Aged crystals	0.72–0.95(5)	3.00	3.4–3.5(2)
Annealed crystals	0.83–0.99(6)	3.00	3.1–3.2(2)
Pristine polycrystals	0.93–1.03(6)	3.00	3.1–3.3(2)
Aged polycrystals	0.72–0.90(6)	3.00	3.2–3.7(2)
Annealed polycrystals	0.79–0.91(5)	3.00	2.9–3.3(2)

of Refs. [12,18], but inconsistent with the direct chemical-composition measurements. Considering the severe broadening of the XRD peaks which point to phase separations in the samples, we conjecture that the K-rich phase is better crystallized (this is very likely, since the K-deficient phase undergoes several chemical processes, leading to poorer crystallinity), which mostly contributes the XRD intensities. In this circumstance, it is not surprising that the Rietveld analysis does not show any signature of the K vacancy.

The above results allow us to figure out the possible phase conversions in the processes of the K deintercalation and the post-treatments. First, the phase conversion from $\text{K}_2\text{Cr}_3\text{As}_3$ to the pristine 133 should accompany the incorporation of hydrogen, according to the neutron diffraction result [18]. Owing to the K content that is close to 1.0, the pristine 133 samples are written as $\text{KCr}_3\text{As}_3\text{H}_y$ (here hydrogen is placed at the end because of its largest negativity, in accordance with the conventional nomenclature for inorganic compounds). Second, the decrease in K content without H_2 gas releasing, and without obvious changes in lattice parameters either, in the aging process strongly suggests an ion exchange between K^+ and H_3O^+ (from the remaining water in ethanol), as shown in Figs. 1(b) and 1(c). This process should be slow especially for the case of crystals because of the necessary diffusions of H_3O^+ and K^+ ions. Third, the H in H_3O^+ enters the $2b$ site in the Cr_3 tubes. This H-intercalation process must overcome the barrier of Cr_3As_3 double walls, which needs a sufficient activation energy. Obviously, the annealing may accelerate the process, finally forming $\text{K}_{1-\delta}\text{Cr}_3\text{As}_3\text{H}_x$ [Fig. 1(d)]. We will return to the issue of the H-intercalation processes in Sec. IV.

B. Aging effect

We mainly employed the magnetic measurement to detect both the spin-glass behavior and the superconducting transition. Figure 3 shows temperature dependence of dc magnetic susceptibility of the 133-type single-crystalline samples together with that of the 233-type crystals for comparison. The as-grown $\text{K}_2\text{Cr}_3\text{As}_3$ crystal shows a sharp superconducting transition at $T_c = 6.1$ K with nearly 100% ZFC diamagnetism

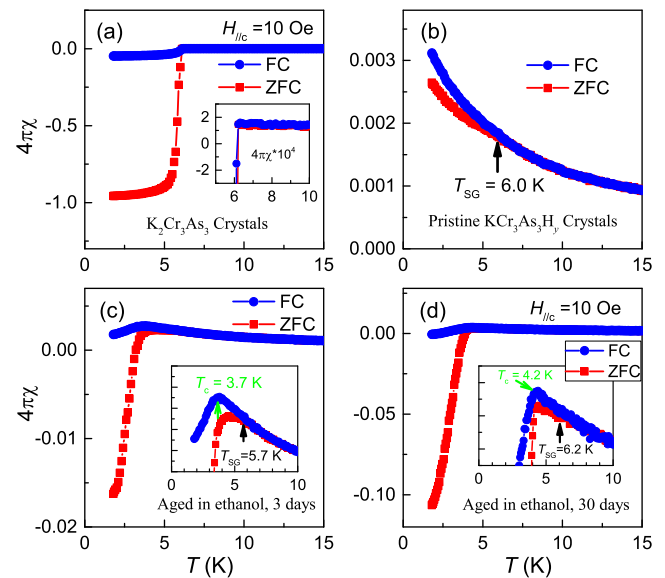


FIG. 3. Temperature dependence of dc magnetic susceptibility (in units of $4\pi\chi$) at low temperatures for the single-crystalline samples of $\text{K}_2\text{Cr}_3\text{As}_3$ (a), pristine $\text{KCr}_3\text{As}_3\text{H}_y$ (b), and $\text{K}_{1-\delta}\text{Cr}_3\text{As}_3\text{H}_x$ aged samples [(c) and (d)]. FC and ZFC denote field cooling and zero-field cooling, respectively. The insets show the close-ups so that the superconducting and spin-glass transitions can be simultaneously seen.

[Fig. 3(a)]. The normal-state susceptibility shown in the inset is basically temperature independent, suggestive of Pauli paramagnetism. For the pristine $\text{KCr}_3\text{As}_3\text{H}_y$, however, superconductivity completely disappears above 1.8 K, and a spin-glass transition shows up at around 6 K with Curie-Weiss (CW) paramagnetism [Fig. 3(b)]. After the pristine sample was aged for 3 days, minor superconductivity at 3.7 K emerges with $\sim 2\%$ ZFC diamagnetism [Fig. 3(c)]. The sample aged for 30 days shows 12% ZFC diamagnetism with an enhanced T_c of 4.2 K [Fig. 3(d)]. The enhancement of superconductivity with aging continues up to one year. The T_c value is 4.5 K with $\sim 50\%$ ZFC diamagnetism for the one-year-aged sample (see Fig. S3(a) in the SM [20]). Note that the spin-glass behavior together with the CW paramagnetism is still present in the aged samples. The simultaneous appearance of spin glass and partial superconductivity further confirms the existence of inhomogeneity or phase separation in the 133-type samples.

The magnetic measurement results for the polycrystalline samples, shown in Fig. 4, bear both similarities and differences in comparison with those of single-crystalline samples above. The similar behaviors include (1) the absence of superconductivity for the pristine $\text{KCr}_3\text{As}_3\text{H}_y$ polycrystals, (2) CW paramagnetism with a spin-glass behavior for all the samples, and (3) the emergence of superconductivity for aged samples. The main difference is that the superconducting diamagnetism is much weaker ($4\pi\Delta\chi \sim 0.5\%$) with lower T_c values, consistent with the previous report [12,18]. The magnetic shielding fraction, represented by $4\pi\chi_{\text{ZFC}}$, even decreased after one-year aging, in sharp contrast with the continuing increase in ZFC diamagnetism for the single-crystalline samples (Fig. S3 in the SM [20]).

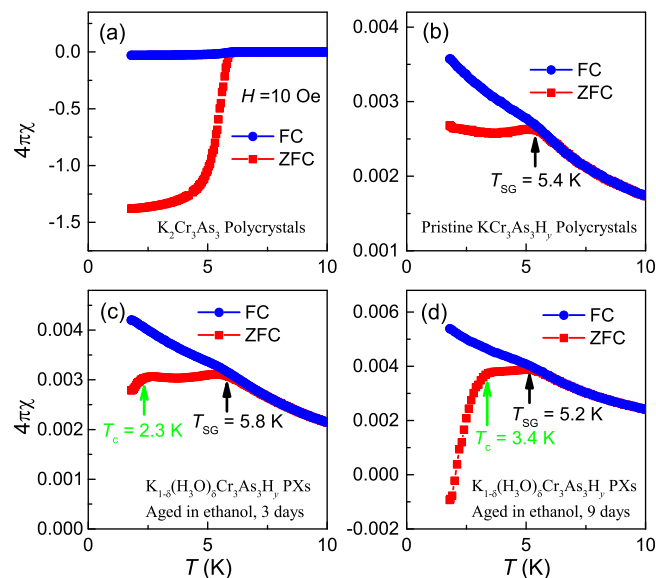


FIG. 4. Temperature dependence of dc magnetic susceptibility at low temperatures for the polycrystalline samples of $\text{K}_2\text{Cr}_3\text{As}_3$ (a), pristine $\text{KCr}_3\text{As}_3\text{H}_y$ (b), and $\text{K}_{1-\delta}(\text{H}_3\text{O})_\delta\text{Cr}_3\text{As}_3\text{H}_y$ aged [(c) and (d)]. FC and ZFC denote field cooling and zero-field cooling, respectively.

C. Annealing effect

Above we demonstrate that superconductivity can be induced simply with increasing aging time for the single-crystalline samples. The T_c values and the ZFC diamagnetism are consistent with those of sample A (soaked in ethanol for one week) in Ref. [15]. It was found that after the ethanol-thermal bath at 80°C followed by annealing at 100°C , the T_c value and the ZFC diamagnetism were increased for both the single crystals and the polycrystals [15,18]. Note that these samples had actually been aged and annealed simultaneously. Below we show the annealing effect for the pristine and the aged samples, respectively.

While the pristine 133-type crystals show a spin-glass behavior without any signature of superconductivity, the annealed crystals exhibit superconductivity at 4.3 K, as shown in Fig. 5(a). Nonetheless, the ZFC diamagnetism is only 4%. For the 30-day-aged crystals, on the other hand, the annealing leads to a higher T_c of 4.8 K and a stronger ZFC diamagnetic signal of 22%. The T_c value is even 0.1 K higher than the counterpart of the ethanol-thermal-treated crystals [15]. The spin-glass behavior is almost invisible above 4.8 K, but the normal state still shows the CW paramagnetism. Assuming Pauli paramagnetism for the superconductor as usual, this result suggests that the sample is still a mixture of superconducting phase and a CW paramagnetic one.

The enhancement of superconductivity by annealing is also seen for the 133-type polycrystals. As is seen in Fig. 6(a), superconductivity emerges at 4.0 K after the nonsuperconducting pristine sample was annealed at 100°C for 12 hours. The ZFC diamagnetism is about 3% at 1.8 K; meanwhile, the spin-glass transition temperature, T_{SG} , increases by 0.6 K. In the case of the 3-day-aged polycrystals, which shows a low T_c of 2.3 K with tiny (0.04%) ZFC diamagnetism, the annealing

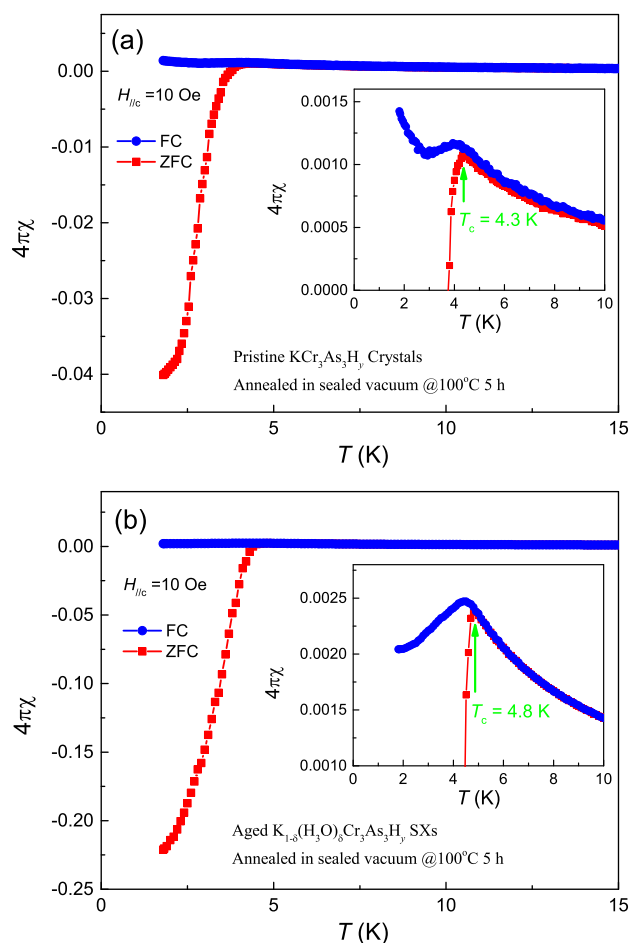


FIG. 5. Temperature dependence of the magnetic susceptibility for the pristine $\text{KCr}_3\text{As}_3\text{H}_y$ (a) and 30-day-aged $\text{K}_{1-\delta}(\text{H}_3\text{O})_\delta\text{Cr}_3\text{As}_3\text{H}_y$ (b) crystals that are post-annealed. The insets show the close-ups for the superconducting transitions.

leads to a remarkable increase in T_c (4.6 K) with a large diamagnetic signal (27%). The T_{SG} value further increases up to 6.4 K. The FC curve abnormally increases with decreasing temperature just below T_c , which is not well understood at the present stage. For the one-year-aged sample, annealing induces a T_c of 4.7 K with 7% ZFC diamagnetism [see the inset of Fig. S3(b)]. The simultaneous enhancements of T_c and T_{SG} seem to be related to the phase separation mentioned above.

Here we should comment on the ZFC diamagnetic signal which actually measures the magnetic shielding fraction, rather than the superconducting volume fraction (SVF). For inhomogeneous samples like the case here, the real SVF is often much smaller than the ZFC diamagnetism. While the ZFC diamagnetism is almost 100% at 2 K for the KCr_3As_3 crystals [15], the superconducting transition is very broad with the deep susceptibility decrease at 3.5 K (much lower than its $T_c = 4.7$ K), in contrast with the sharp transition in $\text{K}_2\text{Cr}_3\text{As}_3$ shown in Fig. 3(a). Indeed, the dimensionless specific-heat jump is only 0.47 [15], which is about 20% of that in $\text{K}_2\text{Cr}_3\text{As}_3$ [1], suggesting a much lower SVF of $\sim 20\%$. For the superconductive 133-type samples in the present study, the ZFC diamagnetism is mostly below 30%, and the

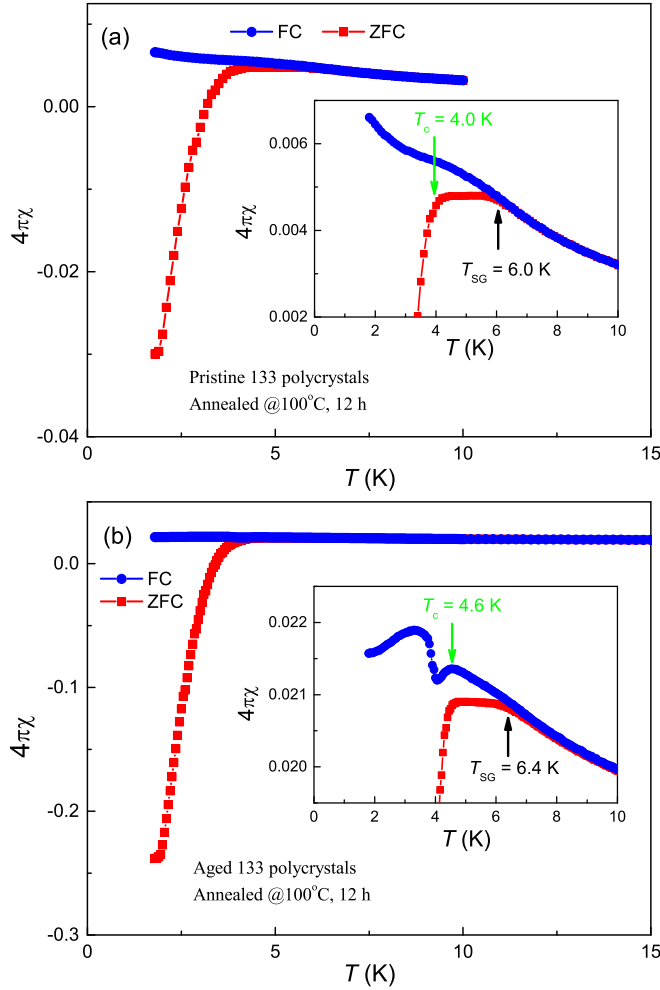


FIG. 6. Temperature dependence of the magnetic susceptibility for the post-annealed $K_{1-\delta}Cr_3As_3H_x$ polycrystals. The insets show the close-ups for the spin-glass and superconducting transitions.

superconducting transition is always broad, indicating even lower SVFs. In this context, the observed superconductivity so far is basically nonbulk in nature, which could be related to the structural and compositional inhomogeneity. A possible conjecture is that superconductivity occurs in the complete $(Cr_3As_3H)_\infty$ chains, while the incomplete $(Cr_3As_3H_x)_\infty$ chains give rise to a spin-glass behavior. If this is the case, we actually observed a columnar superconductivity, as opposed to granular superconductivity, in the present quasi-one-dimensional system.

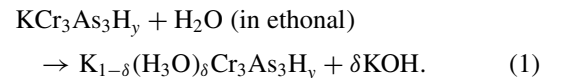
Note that neutron diffraction actually supplies information of an average structure. As concluded by Taddei *et al.* [18], the enhancement or appearance of superconductivity is due to the additional H intercalation. It was also found that the lattice parameter c of the superconductive samples is relatively larger. Figure S4 plots T_c and ZFC diamagnetism as functions of the c parameter for the 133-type polycrystalline samples. Consistently, both T_c and ZFC diamagnetism tend to increase with the c axis. The increase in c should be associated with the H intercalation, according to Ref. [18]. The increase for the H occupancy naturally increases the SVF, if one assumes that

superconductivity only occurs in the complete $(Cr_3As_3H)_\infty$ chains.

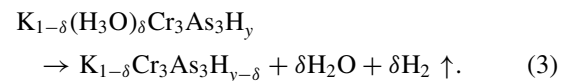
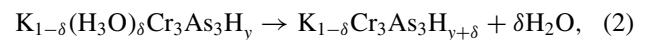
IV. DISCUSSION

The results above show that the pristine 133 samples are not superconducting, and superconductivity is actually induced by the aging or annealing process. On the whole, the aging and annealing effects can be understood in terms of the H intercalation [18]. In the pristine $KCr_3As_3H_y$, the H occupancy is not enough for superconductivity. With the aging or annealing, more H is introduced, and superconductivity emerges in $K_{1-\delta}Cr_3As_3H_x$. Nevertheless, why is the aging effect so different for the single crystals and the polycrystals? At first sight, the difference in the specific surface area (SSA) between polycrystals and single crystals, which yields a different surface adsorption effect, seems to be relevant. However, the adsorption of H_2 is actually insignificant from the measurement of hydrogen gas released. Furthermore, even if considering the relatively large SSA for the adsorption of hydrogen in the polycrystals, one concludes that the polycrystals would have a more remarkable aging effect, which is the opposite of the experimental fact.

Before understanding the different aging effect for the crystals and polycrystals, one needs to know how H enters the Cr_3 tubes. First, $K_2Cr_3As_3$ rapidly reacts with C_2H_5OH , forming a nearly stoichiometric 133 compound. The process involves the release of hydrogen gas; thus some hydrogen atoms reasonably enter the Cr_3 tubes, forming $KCr_3As_3H_y$ [Fig. 1(b)]. The y value was estimated to be 0.08 from the measurement of the H_2 volume for a polycrystalline sample (see Fig. S1 in the SM [20]). Second, the K content decreases without appreciable H_2 releasing in the process of aging. This phenomenon points to an ion exchange reaction between K^+ and H_3O^+ in the ethanol bath (ethanol always contains a small amount of water), similar to the case in a cobalt oxyhydrate superconductor [21], forming an intermediate compound, $K_{1-\delta}(H_3O)_\delta Cr_3As_3H_y$ [Fig. 1(c)]:



The intermediate compound subsequently undergoes the following two competitive reactions:



Equation (3) was derived from the aforementioned observations: (1) When the pristine polycrystals are soaked in water, H_2 bubbles escape from the liquid; and (2) exposure of the dried pristine polycrystals in humid air releases a large amount of heat [in humid air, Eq. (1) proceeds]. The two phenomena coincidentally suggest that the internal process, $H^+ + H^- \rightarrow H_2$ ($\Delta H^0 = -17.37$ eV) [22], takes place spontaneously (the hydrogen in the Cr_3 tubes is demonstrated to be in a valence state of -1 by the first-principles calculations [19]). Intuitively, Eq. (3) proceeds if δ and y are simultaneously large enough. In Eq. (2), the internal migration of hydrogen from

the K-site H_3O^+ to the $2b$ site within the Cr_3 tubes generally needs a considerably high activation energy, which makes the H-intercalation reaction relatively slow. That is why annealing is more effective to introduce superconductivity.

Note that the H content in the Cr_3 tubes increases via Eq. (2), yet it decreases according to Eq. (3). Taking this information in mind, one may understand the different aging effect for the crystals and polycrystals. As we know, the basic difference between crystals and polycrystals is the crystallite size. The single crystals are mainly 50–200 μm in thickness, while the crystallites in polycrystals are 1–2 μm thick. Equation (1) starts at the solid-liquid interface, and the reaction proceeds with the diffusions of H_2O , H_3O^+ , K^+ , and OH^- . For the single crystals, the diffusion length is much longer; thus the ion-exchange process goes much more slowly. This allows the crystals to keep the δ value in the intermediate compound at a lower level, such that Eq. (3) will not take place basically. In the case of polycrystals, Eq. (1) proceeds faster, leading to a relatively large δ value, and the H content cannot reach a high value because Eq. (3) reduces the H occupancy. Even if Eq. (3) does not take place, the intercalated H content, $y + \delta$, according to Eq. (2), will not be so high ($y \approx 0.1\text{--}0.3$, $\delta \approx 0.2$). This could explain the very low SVFs in $\text{K}_{1-\delta}\text{Cr}_3\text{As}_3\text{H}_x$ ($\delta \approx 0.2$, $x \approx 0.3\text{--}0.5$) as estimated above.

The annealing effect can also be explained with the H-intercalation mechanism depicted in Fig. 1. For the pristine samples in which a small number of H_3O^+ ions already exist, the annealing may introduce superconductivity, but the enhancement of superconductivity is limited by the relatively less H intercalation. In the case of aged samples, superconductivity is enhanced more remarkably because there are more H_3O^+ ions which leads to more H intercalation for the annealed sample.

V. CONCLUDING REMARKS

In summary, we have studied the aging and annealing effect on the structural, compositional, and physical properties in

the 133-type $\text{K}_{1-\delta}\text{Cr}_3\text{As}_3\text{H}_x$ system. The results show that the pristine 133 crystals and polycrystals only exhibit a spin-glass behavior without any superconducting transition. Superconductivity is induced with aging in ethanol and/or annealing at about 100 °C. Nevertheless, the superconducting transition is very broad, and the superconducting volume fraction is quite low (at most 20%). Meanwhile, the spin-glass behavior is mostly maintained with CW paramagnetism, suggesting a phase separation scenario. The phase separation is probably related to the compositional inhomogeneity with K deficiency at a micrometer scale, which accounts for the XRD-peak broadening.

The aging and annealing effects can be consistently explained by the phase conversions from $\text{K}_2\text{Cr}_3\text{As}_3$ to non-superconducting $\text{KCr}_3\text{As}_3\text{H}_y$, and finally to superconducting $\text{K}_{1-\delta}\text{Cr}_3\text{As}_3\text{H}_x$ ($\delta \approx 0.2$, $x \approx 0.3\text{--}0.5$). The ion exchange between K^+ and H_3O^+ seems to be a necessary intermediate process for the H intercalation, which explains the different aging effect between single crystals and polycrystals. It is of great interest for the future to synthesize the ideal H-fully-occupied phase, $\text{KCr}_3\text{As}_3\text{H}$. One could expect bulk superconductivity in this “1331”-type material. Another interesting issue is how the spin-glass phase changes into the superconducting state, as mentioned by Taddei *et al.* [18]. The last issue concerns the ground state of the hydrogen-free KCr_3As_3 . Is it still a spin glass, or is it with or without any magnetic ordering at low temperatures [14,23,24]? Future studies addressing these questions are highly desirable.

ACKNOWLEDGMENTS

This work was supported by the National Natural Science Foundation of China (Grants No. 11674281 and No. 11804302), the National Key Research and Development Program of China (2017YFA0303002), and the Fundamental Research Funds for the Central Universities of China (2019FZA3004).

-
- [1] J.-K. Bao, J.-Y. Liu, C.-W. Ma, Z.-H. Meng, Z.-T. Tang, Y.-L. Sun, H.-F. Zhai, H. Jiang, H. Bai, C.-M. Feng, Z.-A. Xu, and G.-H. Cao, Superconductivity in Quasi-One-Dimensional $\text{K}_2\text{Cr}_3\text{As}_3$ with Significant Electron Correlations, *Phys. Rev. X* **5**, 011013 (2015).
- [2] G.-H. Cao, J.-K. Bao, Z.-T. Tang, Y. Liu, and H. Jiang, Peculiar properties of Cr_3As_3 -chain-based superconductors, *Philos. Mag.* **97**, 591 (2017).
- [3] R. Y. Chen and N. L. Wang, Progress in Cr- and Mn-based superconductors: A key issues review, *Rep. Prog. Phys.* **82**, 012503 (2018).
- [4] X. Wu, F. Yang, C. Le, H. Fan, and J. Hu, Triplet p_z -wave pairing in quasi-one-dimensional $\text{A}_2\text{Cr}_3\text{As}_3$ ($A = \text{K}, \text{Rb}, \text{Cs}$), *Phys. Rev. B* **92**, 104511 (2015).
- [5] Y. Zhou, C. Cao, and F.-C. Zhang, Theory for superconductivity in alkali chromium arsenides $\text{A}_2\text{Cr}_3\text{As}_3$ ($A = \text{K}, \text{Rb}, \text{Cs}$), *Sci. Bull.* **62**, 208 (2017).
- [6] H. Zhong, X.-Y. Feng, H. Chen, and J. Dai, Formation of Molecular-Orbital Bands in a Twisted Hubbard Tube: Implications for Unconventional Superconductivity in $\text{K}_2\text{Cr}_3\text{As}_3$, *Phys. Rev. Lett.* **115**, 227001 (2015).
- [7] J. Yang, Z. T. Tang, G. H. Cao, and G.-q. Zheng, Ferromagnetic Spin Fluctuation and Unconventional Superconductivity in $\text{Rb}_2\text{Cr}_3\text{As}_3$ Revealed by As-75 NMR and NQR, *Phys. Rev. Lett.* **115**, 147002 (2015).
- [8] J. Luo, J. Yang, R. Zhou, Q. G. Mu, T. Liu, Z.-a. Ren, C. J. Yi, Y. G. Shi, and G.-q. Zheng, Tuning the Distance to a Possible Ferromagnetic Quantum Critical Point in $\text{A}_2\text{Cr}_3\text{As}_3$, *Phys. Rev. Lett.* **123**, 047001 (2019).
- [9] Z.-T. Tang, J.-K. Bao, Y. Liu, Y.-L. Sun, A. Ablimit, H.-F. Zhai, H. Jiang, C.-M. Feng, Z.-A. Xu, and G.-H. Cao, Unconventional superconductivity in quasi-one-dimensional $\text{Rb}_2\text{Cr}_3\text{As}_3$, *Phys. Rev. B* **91**, 020506(R) (2015).
- [10] Z.-T. Tang, J.-K. Bao, Z. Wang, H. Bai, H. Jiang, Y. Liu, H.-F. Zhai, C.-M. Feng, Z.-A. Xu, and G.-H. Cao, Superconductivity in quasi-one-dimensional $\text{Cs}_2\text{Cr}_3\text{As}_3$ with large interchain distance, *Sci. China Mater.* **58**, 16 (2015).

- [11] Q.-G. Mu, B.-B. Ruan, B.-J. Pan, T. Liu, J. Yu, K. Zhao, G.-F. Chen, and Z.-A. Ren, Ion-exchange synthesis and superconductivity at 8.6 K of $\text{Na}_2\text{Cr}_3\text{As}_3$ with quasi-one-dimensional crystal structure, *Phys. Rev. Mater.* **2**, 034803 (2018).
- [12] J.-K. Bao, L. Li, Z.-T. Tang, Y. Liu, Y.-K. Li, H. Bai, C.-M. Feng, Z.-A. Xu, and G.-H. Cao, Cluster spin-glass ground state in quasi-one-dimensional KCr_3As_3 , *Phys. Rev. B* **91**, 180404(R) (2015).
- [13] Z.-T. Tang, J.-K. Bao, Y. Liu, H. Bai, H. Jiang, H.-F. Zhai, C.-M. Feng, Z.-A. Xu, and G.-H. Cao, Synthesis, crystal structure and physical properties of quasi-one-dimensional ACr_3As_3 ($A = \text{Rb}, \text{Cs}$), *Sci. China Mater.* **58**, 543 (2015).
- [14] Y. Feng, X. Zhang, Y. Hao, A. D. Hillier, D. T. Adroja, and J. Zhao, Magnetic ground state of KCr_3As_3 , *Phys. Rev. B* **99**, 174401 (2019).
- [15] Q.-G. Mu, B.-B. Ruan, B.-J. Pan, T. Liu, J. Yu, K. Zhao, G.-F. Chen, and Z.-A. Ren, Superconductivity at 5 K in quasi-one-dimensional Cr-based KCr_3As_3 single crystals, *Phys. Rev. B* **96**, 140504(R) (2017).
- [16] T. Liu, Q.-G. Mu, B.-J. Pan, J. Yu, B.-B. Ruan, K. Zhao, G.-F. Chen, and Z.-A. Ren, Superconductivity at 7.3 K in the 133-type Cr-based RbCr_3As_3 single crystals, *Europhys. Lett.* **120**, 27006 (2017).
- [17] H. Zuo, J.-K. Bao, Y. Liu, J. Wang, Z. Jin, Z. Xia, L. Li, Z. Xu, J. Kang, Z. Zhu, and G.-H. Cao, Temperature and angular dependence of the upper critical field in $\text{K}_2\text{Cr}_3\text{As}_3$, *Phys. Rev. B* **95**, 014502 (2017).
- [18] K. M. Taddei, L. D. Sanjeewa, B.-H. Lei, Y. Fu, Q. Zheng, D. J. Singh, A. S. Sefat, and C. dela Cruz, Tuning from frustrated magnetism to superconductivity in quasi-one-dimensional KCr_3As_3 through hydrogen doping, [arXiv:1905.03360](https://arxiv.org/abs/1905.03360).
- [19] S.-Q. Wu, C. Cao, and G.-H. Cao, Lifshitz transition and nontrivial H-doping effect in the Cr-based superconductor $\text{KCr}_3\text{As}_3\text{H}_x$, *Phys. Rev. B* **100**, 155108 (2019).
- [20] See Supplemental Material at <http://link.aps.org/supplemental/10.1103/PhysRevMaterials.3.114802> for additional experimental data (with four figures and two tables), including the compositional measurement by EDXS.
- [21] G. H. Cao, X. M. Tang, Y. Xu, M. Zhong, X. Z. Chen, C. M. Feng, and Z. A. Xu, Proton incorporations and superconductivity in a cobalt oxyhydrate, *Solid State Commun.* **131**, 125 (2004).
- [22] W. Grochala and P. P. Edwards, Thermal decomposition of the non-interstitial hydrides for the storage and production of hydrogen, *Chem. Rev.* **104**, 1283 (2004).
- [23] C. Cao, H. Jiang, X.-Y. Feng, and J. Dai, Reduced dimensionality and magnetic frustration in KCr_3As_3 , *Phys. Rev. B* **92**, 235107 (2015).
- [24] G. Xing, L. Shang, Y. Fu, W. Ren, X. Fan, W. Zheng, and D. J. Singh, Structural instability and magnetism of superconducting KCr_3As_3 , *Phys. Rev. B* **99**, 174508 (2019).